Agricultural Water Management 243 (2021) 106429

Contents lists available at ScienceDirect

Agricultural Water Management

journal homepage: www.elsevier.com/locate/agwat

Modeling the response of dry bean yield to irrigation water availability controlled by watershed hydrology

R. Mompremier[a], Y. Her[b,*], G. Hoogenboom[a,c], K. Migliaccio[a], R. Muñoz-Carpena[a], Z. Brym[d], R.W. Colbert[e,f,g], W. Jeune[e,f]

[a] Department of Agricultural and Biological Engineering, Institute of Food and Agricultural Sciences, University of Florida, Gainesville, USA
[b] Department of Agricultural and Biological Engineering / Tropical Research and Education Center, Institute of Food and Agricultural Sciences, University of Florida, Gainesville, USA
[c] Institute for Sustainable Food Systems, University of Florida, Gainesville, USA
[d] Department of Agronomy / Tropical Research and Education Center, Institute of Food and Agricultural Sciences, University of Florida, Gainesville, USA
[e] Feed the Future Haiti-AREA, University of Florida, Institute of Food and Agricultural Sciences, Gainesville, FL, USA
[f] Faculté des Sciences de l'Agriculture et de l'Environnement, Université Quisqueya, 218, Port-au-Prince, Haïti
[g] Departamento de Ciencia y Producción Agropecuaria, Escuela Agrícola Panamericana-Zamorano, Tegucigalpa, Honduras

ARTICLE INFO

Keywords:
Crop growth
Water resources
Crop modeling
DSSAT
Watershed monitoring
Haiti

ABSTRACT

The effectiveness of agricultural productivity is dependent on the availability of ambient natural resources as well as on the efficiency of on-site management practices. The overall understanding of a production system can help with finding management options that enable for the available resources to be used more efficiently and thus improving productivity. We investigated the response of dry bean (*Phaseolus vulgaris L*) yield to water availability in an irrigation district controlled by off-site hydrology to show how integrated knowledge can benefit agricultural production. This study focused on an agricultural system where an upstream watershed provided water for dry bean production in its downstream irrigation district in Haiti. Dry bean growth was mathematically represented using the Cropping System Model (CSM)-CROPGRO-Dry bean model of the Decision Support System for Agrotechnology Transfer (DSSAT). The upstream runoff was measured to quantify irrigation water availability changes over time. The cultivar parameters of the dry bean model were calibrated to minimize differences between simulated and observed dry bean growth and yield. The model was then used to determine long-term dry bean response to water availability scenarios, including fifteen combinations of five growing periods and three irrigation conditions. The results showed that dry bean productivity was closely associated with the upstream watershed hydrology and that growing dry bean earlier than the standard management scenario (December to March) increased predicted dry bean yield by over 80 % with the available water resources and associated temporal variability. These findings indicate that an integrated systems approach could improve dry bean production by identifying alternative management practices to use the available water more efficiently.

1. Introduction

Limited water availability is one of the critical challenges that farmers face in developing countries such as Haiti (Laraus, 2004; Molnar et al., 2015; Yang and Zehnder, 2002). At a global scale, the agricultural sector is the largest user of freshwater resources, with surface water that is readily accessible but highly variable in time and location as the main source for irrigation in many areas (Dieter, 2018; FAO, 2017, 2011; OECD, 2017; Stubbs, 2016; Winter et al., 1998). The availability of surface water for irrigation depends on precipitation, hydrological processes such as runoff generation and transport, and their spatial-temporal variability. Therefore, agricultural production and productivity are directly impacted by surface water hydrology (McNider et al., 2015; Wallender and Grismer, 2002). For instance, there is insufficient water for farmers to grow dry bean (*Phaseolus vulgaris L*) during the growing season (December to March) since the source of irrigation, i.e., streamflow, is limited during this season in Haiti. In addition, agricultural decisions such as the planting date are frequently determined without the guidance of scientific studies and practical evidence (Alvarez and Nuthall, 2006; McCown, 2002;

* Corresponding author at: 18905 SW 280th St., Homestead, FL 33031, USA.
E-mail address: yher@ufl.edu (Y. Her).

https://doi.org/10.1016/j.agwat.2020.106429
Received 3 April 2020; Received in revised form 21 July 2020; Accepted 31 July 2020

Shackelford et al., 2019). This traditional management practice might be the result of a balance among various factors, including rainfall, temperature, and workability that influence crop growth and management, but the trade-offs have not been explored sufficiently to guide management practices for improved efficiency of agricultural management.

Several studies have shown that the fluctuations in crop production are often due to the variability in rainfall and extreme events such as drought and flooding (Gornall et al., 2010; Guan et al., 2015; Olayide et al., 2016). In Haiti, for instance, downstream agricultural areas are closely connected to upstream areas, creating a unique rural landscape along the coastal lines. The mountainous catchments serve as the source of irrigation water for low-lying crop areas, thus water collected from upstream plays a critical role for agricultural production. In this interconnected system an understanding of watershed hydrology is essential for improved crop production. However, the connection between two areas, upstream mountainous catchment and downstream agriculture, has not been studied sufficiently to guide watershed management practices for improved sustainability of agriculture.

Integrated knowledge and a system approach are instrumental in improving the efficiency of managing natural resources (Brodt et al., 2011; Duan et al., 2018; ICID, 2017; Nepal et al., 2014; Sayer and Cassman, 2013; Yoon et al., 2015). An understanding of the relationship between upstream and downstream areas is necessary for efficient resource management such as flood control, water quality improvement, and biodiversity (McNider et al., 2015; Wallender and Grismer, 2002; Wang et al., 2016). From a holistic point of view, the lack of water in an upstream watershed may reduce agricultural production in a downstream area. Past studies have shown that forested areas could stabilize the flow regime by increasing the baseflow, which would increase water availability during the dry period (Belmar et al., 2016; Gashaw et al., 2017; Sun et al., 2005). Similarly, Gebremicael et al. (2019) found that forested areas increased dry-season streamflow and decreased wet-season flow while deforested areas had the opposite effect on streamflow. The decrease in crop production can then lead to farmers finding other sources of income by harvesting timber in the upstream watershed, which reduces the number of trees (or forest areas) in the water source area and then decreases water availability to the downstream area and thus agricultural productivity. However, this results in a vicious cycle; implementing agricultural management practices to increase productivity with limited water can reduce the occurrence of such negative feedback cycles.

The overall goal of this study was to investigate the linkage between upstream, i.e., the source of irrigation water, and downstream agricultural areas to provide the information required to make efficient management decisions for improved crop production. The specific objectives of this study were (1) to assess the temporal variation of water available for the dry bean growing season, (2) to evaluate the crop genetic coefficients for the CSM(cropping system model)-CROPGRO-Dry bean model, and then (3) to determine dry bean response to water availability for different growing season and irrigation practices. This study also discussed the implications of the results and their limitations associated with the quality and quantity of data used in the modeling experiment.

2. Methods and materials

2.1. Study areas

The Arcahaie region (18° 55′ 00″ N and 72° 33′ 20″ W) is located 41 km northwest from the capital of Haiti, Port-au-Prince (Fig. 1). The Courjolle River is one of the rivers that flows from the mountainous watersheds (north) to low-lying coastal areas (south) in the region. The Courjolle River watershed is characterized by hills and mountains with high elevation, draining water from 80 km^2 to its downstream agricultural areas. A geospatial analysis with the 30-m Shuttle Radar Topography Mission (SRTM) digital elevation model (DEM) obtained from the United States Geological Survey (USGS, 2019) showed that the elevation of the watershed ranges from 100 m to 1,498 m with a mean elevation of 779 m above the mean sea level and a mean slope of 34.5 %. According to the recent land use data obtained from the Centre National de l'Information Géo-Spatiale (CNIGS), the watershed is mostly covered by savanna (95 %) with dense forestry (2 %) and other unclassified plants (3 %). The soil in the watershed has been characterized as silty clay loam, sandy loam, and clay loam (FAO-UNESCO, 2003).

Fig. 1. The watershed and agricultural system of this study located in Arcahaie, Haiti. The land use and Haiti boundary data were obtained from the CNIGS, Haiti.

The upstream watershed and downstream agricultural areas are connected by a concrete dam known as the Courjolle River dam, which is used to provide water to the downstream irrigation areas and the dry bean fields (Fig. 1). The water, controlled by gates, is diverted into two primary canals that pass through the irrigation areas. Dry bean is grown from December to March and irrigated with water discharged from the Courjolle River. In the irrigated areas, the dry bean fields are flooded using a furrow method, which is subject to water losses by evaporation, infiltration, and percolation. The irrigation canals are not well maintained, which exacerbates the losses during the water transport process.

The climate of the Arcahaie region is classified as a tropical wet-dry climate (Aw) according to the Köppen classification, which is characterized by distinct wet and dry seasons and precipitation occurring during the summer season (Peel et al., 2007). The mean annual rainfall is 928 mm based on historical records from 1981 to 2017 (Dinku et al., 2018; Funk et al., 2015). The region has two distinct wet periods, April to June and August to November, while the air is relatively dry between December and February (Fig. 2). The average annual temperature from 1984 and 2018 was approximately 27.9 °C. August and January are the warmest and coolest months, with an average temperature of 29.6 °C and 26.2 °C, respectively (Fig. 2) (Maldonado et al., 2019).

Fig. 2. Long-term average monthly rainfall, solar radiation, and temperature from NASA POWER (1984–2018) daily data for Arcahaie, Haiti. The error bars represent the variability of the monthly rainfall and temperatures over the 34 years.

The dry bean is one of the most widely-cultivated staple crops in the world. It is a complete source of nutrition, containing significantly more protein, fiber, iron, potassium, and folic acid than conventional grains such as wheat, oats, and other cereals (Siddiq et al., 2010). Dry bean is also important to the Haitian population as a source of iron and as part of traditional Haitian dishes (FEWS NET, 2018). However, there is high variability in reported dry bean yield. According to FAO Statistics, dry bean yield in Haiti ranged from 400 kg ha^{-1} in 1961 to 697 kg ha^{-1} in 2017 (FAO, 2019). A survey conducted by the Ministry of Agriculture in 2013 showed a higher yield ranging from 1500 to 2000 kg ha^{-1} compared to the FAO Statistics (Inozile, 2016). In 2016, the Haitian Ministry of Agriculture reported an annual dry bean yield of 360 kg ha^{-1} for the western and 450 kg ha^{-1} for the northeastern region of Haiti (USAI/MARNDR, 2016), which are 44 % and 51 % of the world dry bean yield for the same year, respectively (FAO, 2019).

2.2. Dry bean simulation model

2.2.1. Input data

The dry bean model CSM-CROPGRO-Dry bean, which is one of the crop simulation models of the Decision Support System for Agrotechnology Transfer (DSSAT; Hoogenboom et al., 2019a, b, 1994; Jones et al., 2003), was used to mathematically represent dry bean. The dry bean model simulates plant growth and development, and the soil and plant water, nitrogen, and carbon biophysical processes, and ultimately predicts crop yield. Previous studies have demonstrated the capability of the dry bean simulation model to predict the time to flowering, physiological maturity, and yield components (de Oliveira

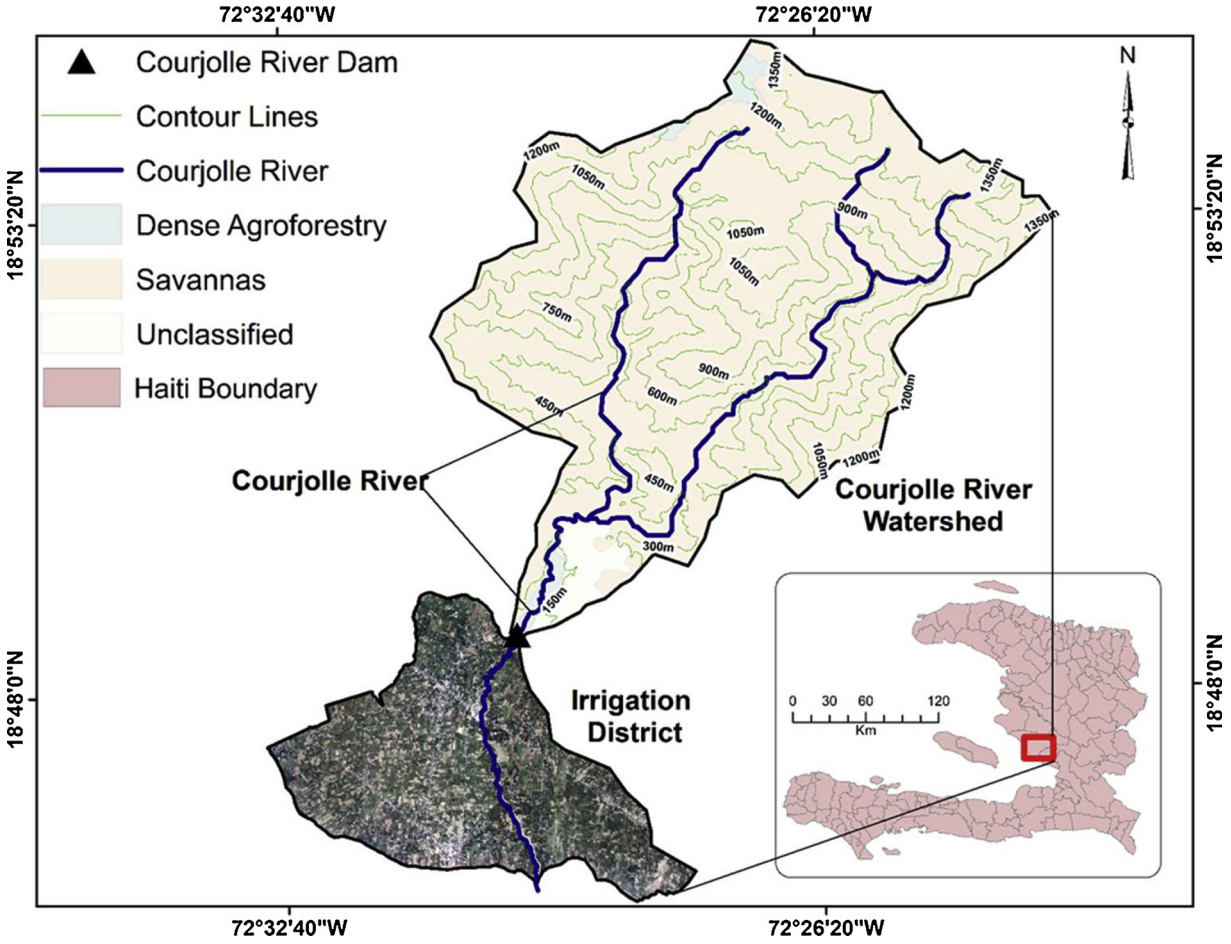

Fig. 1. The watershed and agricultural system of this study located in Arcahaie, Haiti. The land use and Haiti boundary data were obtained from the CNIGS, Haiti.

et al., 2012d; Santos et al., 2016). Weather data from NASA Prediction of Worldwide Energy Resource (POWER) (Stackhouse et al., 2018), soil data from (Jeune, 2015), and crop management data from unpublished experiments (Raphael Colbert, personal communication) served as input data. The model was calibrated and evaluated using experimental data that included dry bean growth, development, and yield measurements in the Arcahaie region. The model was then used to determine the impact of growing season selection and irrigation water availability on dry bean yield and water use efficiency using the seasonal analysis program of DSSAT (Thornton and Hoogenboom, 1994). The irrigation and water availability scenarios were developed based on streamflow discharge hydrographs observed at the outlet of the

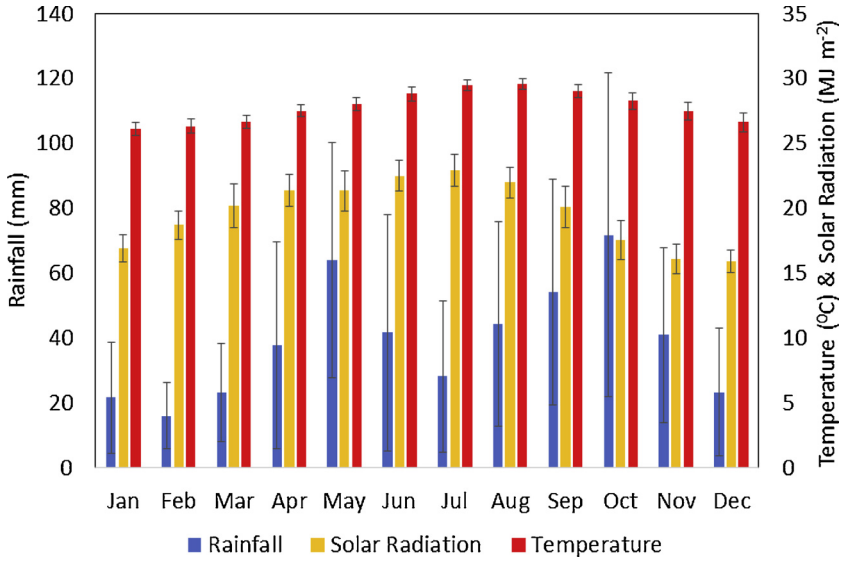

Fig. 2. Long-term average monthly rainfall, solar radiation, and temperature from NASA POWER (1984 – 2018) daily data for Arcahaie, Haiti. The error bars represent the variability of the monthly rainfall and temperatures over the 34 years.

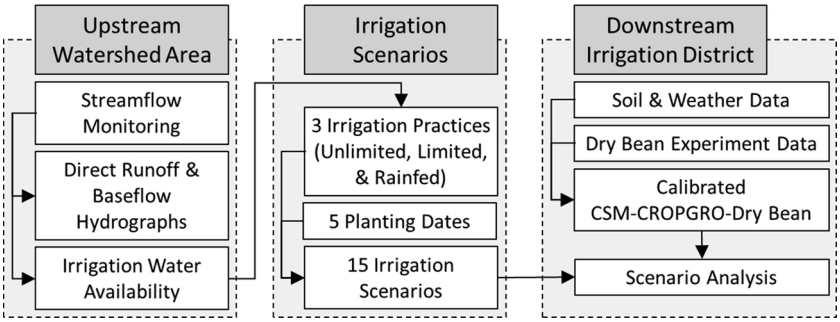

Fig. 3. Overall procedures for evaluating the linkage between the watershed area and irrigation district.

Table 1
Soil characteristics of the dry bean fields in the Arcahaie region, Haiti (Jeune, 2015).

Depth (cm)	Silt (%)	Clay (%)	pH	CEC (cmol/kg)	Organic Matter (%)	Soil Color (Munsell)
0 – 10	54	31	8.0	22.89	2.91	Pale Red (2.5Y 6/2)
10 – 22	59	28	7.7	27.50	2.53	Pale Red (2.5Y 6/2)
22 – 34	56	32	8.0	24.80	2.22	Light Reddish Brown (2.5Y 6/4)
34 – 45	58	32	7.6	27.84	1.27	Light Reddish Brown (2.5Y 6/4)

upstream watershed from August 2018 to April 2019. The overall procedures for this study are summarized in Fig. 3.

Fig. 3. Overall procedures for evaluating the linkage between the watershed area and the irrigation district.

Soil data were obtained from a soil survey conducted by Jeune (2015), which covered the jurisdictional boundaries of the West Department of Haiti, including the Arcahaie region (Table 1). The soil survey data were used to represent the soil characteristics of the study area, such as soil texture (percentage sand, silt, and clay), bulk density, soil organic matter, pH, and the Cation Exchange Capacity (CEC) for each soil horizon. The soil data were also used to determine some of the parameters that control the dynamics of the soil water balance of the crop model (Ritchie, 1998), such as the drained upper limit (DUL), the lower limit of plant available soil water (LL), and saturated soil water content (SAT).

Table 1. Soil characteristics of the dry bean fields in the Arcahaie region, Haiti (Jeune, 2015).

The crop model also requires daily weather data, including precipitation (mm), minimum and maximum air temperature (°C), and solar radiation (MJ m^{-2}), as input. The weather data were collected from two different sources: a local weather station and the remotely sensed rainfall estimates of NASA. The local station is managed by the Unité Hydro Météorologique (Hydro Weather Unit), which is an autonomous Haitian government unit that works with the Ministry of Agriculture, Natural Resources and Rural Development. The weather data were used to calibrate and evaluate the CSM-CROPGRO-Dry bean model from September 1, 2016, to December 20, 2018. As the weather data have only been monitored at the local weather station since 2016, they could not show the long-term trend of weather. Long-term (1983–2018) daily rainfall, daily maximum and minimum temperature, and solar radiation were obtained from NASA POWER (accessible at https://power.larc.nasa.gov/data-access-viewer/) for the scenario analysis. The NASA POWER portal provides daily weather data (maximum and minimum temperature, rainfall, solar radiation) at a spatial resolution of 0.5° × 0.5° (Stackhouse et al., 2018); this system provides agro-meteorological data for the entire globe to compensate for regions where long-term weather data are not readily available (Maldonado et al., 2019). The NASA POWER data have shown to be beneficial to agricultural research (White et al., 2008). Although the remotely sensed weather data are useful for studies especially in developing countries where long-term weather observation data are not common, they include errors as their biases have not been corrected using local observations specific to the study area, which could be one of the potential sources of uncertainty in this study.

2.2.2. Crop model calibration and evaluation

Calibration of the crop system model (CSM) refers to the estimation of crop genetic coefficients (or cultivar-specific parameters) (Boote et al., 2003; Hunt et al., 2001; Jones et al., 1986; Jones et al., 2011). The cultivar coefficients define the traits of each cultivar in the DSSAT modeling ecosystem, and they need to be estimated to represent the local cultivars or varieties (Buddhaboon et al., 2018; Hoogenboom et al., 2019b). In this study, nine cultivar coefficients directly associated with dry bean development and yield were selected for calibration, including EM-FL (time between plant emergence and flower appearance, R1), FL-SD (time between first flower and first seed, R5), SD-PM (time between first seed (R5) and physiological maturity (R7)), SLAVR (specific leaf area of cultivar under standard growth conditions), SIZLF (maximum size of full leaf, three leaflets), WTPSD (maximum weight per seed), SFDPUR (seed filling duration for pod cohort at standard growth conditions), SDPDV (average seeds per pod under standard growing conditions), and PODUR (time required for a cultivar to reach final pod load under optimal conditions).

The CSM-CROPGRO-Dry bean model was calibrated using dry bean growth measurements obtained from field experiments conducted from 2016 to 2018 (Raphael Colbert, personal communication). Detailed information on dry bean management practices used for model calibration and evaluation is shown in Table 2. The variables measured during the experiments included: Anthesis date (ADAP), Maturity date (MDAP), Yield at harvest maturity (HWAM), seed size at harvest maturity (HWUM), and the number of seeds at harvest maturity (no/unit) (H#UM). The quantity, quality, and uncertainty of the dry bean experimental data might vary over years; thus, we devised four different approaches to improve the reliability of the model calibration and evaluation: (1) aggregate all measurements and then randomly split the data into two groups for calibration and evaluation (hereafter differential split-sample test or APP1), which is called APP1-COMB1 when using the first group of measurements for calibration and the second one for evaluation and APP1-COMB2 when using the second group for calibration and the first one for evaluation), (2) use the data collected in 2016 and 2017 for calibration and 2018 for evaluation (APP2), (3) use the data collected in 2016 and 2018 for calibration and 2017 for evaluation (APP3), and (4) use the data collected in 2016 for calibration and 2017 for evaluation (APP4).

Table 2. Dry bean management practices that were used for model calibration and evaluation. The initials soil conditions and water applications were assumed based on the knowledge of local soils and management practices (data were collected by Raphael Colbert).

The differential split-sample test (APP1) has been implemented to ensure the reliability of a calibrated model in hydrological modeling,

Table 2
Dry bean management practices that were used for model calibration and evaluation. The initials soil conditions and water applications were assumed based on the knowledge of local soils and management practices (data were collected by Raphael Colbert).

Period	Item	Description
Common management to the three experiments	Field design	(1) plant population at sowing date: 16.67 plants m^{-2} (2) row spacing: 60 cm (3) planting depth: 4 cm
	Initial soil conditions	(1) Previous crop: Dry bean (2) initial residue root weight: 1 kg ha^{-1} (3) the initial nodule weight: 0 kg ha^{-1} (4) the initial residue Nitrogen: 0.5 % (5) the initial residue Phosphorus: 0.5 % (6) the initial available soil water: 50 % (7) the initial soil Nitrogen: 25 kg ha^{-1}
	Water Applications	24 mm of water every 8 days
2016	Planting date	January 4th, 2016
	Fertilization	(1) 550 kg ha^{-1} of 12-12-20 (12 % of Nitrogen, 12 % of P2O5, and 20 % of K2O) (2) 228.26 kg ha^{-1} of Triple Superphosphate
2016 – 2017	Planting date	December 20th, 2016
	Fertilization	(1) 130.21 kg ha^{-1} of urea (46-0-0) (46 % of Nitrogen) (2) 217.8 kg ha^{-1} of triple super phosphate
2017 – 2018	Planting date	December 21st, 2017
	Fertilization	No fertilization applied

but this methodology is not common in crop modeling (Klemeš, 1986; Gao et al., 2020). In addition, common approaches for crop model calibration and evaluation recommend the use of independent field experiment datasets and treatments that have not suffered from either water or nutrients stresses (Hoogenboom et al., 2019b). However, the quantity (and quality) of dry bean growth observations varied highly over the years, which made the split-sample test a potential alternative to the traditional crop model calibration approaches. For the test (APP1), dry bean experiment data, including the time to flowering, physiological maturity, and yield records from the three years of experiments were randomly selected and split into two groups where each group was comprised of 19 records. The nine cultivar coefficients were then calibrated using one of the groups, and the other group was used to evaluate the performance of the calibrated model and vice versa. In this study, the calibration practices implemented with the first and second halves of the yield data were denoted as combination 1 and combination 2 (COMB1 and COMB2), respectively.

The GLUE framework is integrated into the DSSAT crop modeling system to assist with the estimation of cultivar coefficients (He et al., 2010, 2009; Jones et al., 2011). In the GLUE procedure, the likelihood function (Eq. 1) is used to evaluate the agreement between observed and modeled variables of interest (He et al., 2010).

$$L[\theta_i | O] = \prod_{j=1}^{M} \frac{1}{\sqrt{2\pi\sigma_o^2}} e^{\left(-\frac{(O_j - S(\theta_i))^2}{2\sigma_o^2}\right)} \quad (1)$$

where θ_i is the ith parameter set, i is the index, and it varies from 1 to N, N is the total number of parameter sets generated by the algorithm, $S(\theta_i)$ is the model output derived from the parameter set θ_i, O is the observation, O_j represents the jth observation of O, σ_o^2 signifies the model errors' variance, and M is the number of observations. (He et al., 2010) and (Jones et al., 2011) have described the details of the DSSAT parameter estimation procedures.

Model accuracy is regarded as "excellent" when the Normalized Root Mean Square Error (NRMSE) is less than 10 % and "good" when the NRMSE is between 10 % and 20 % (Anar et al., 2019; Jamieson et al., 1991; Rinaldi et al., 2003). This study identified a parameter set that provided a lower NRMSE than other parameter sets while exhibiting "good" or "excellent" performance in the evaluation period. In the study, the relative error statistic (RE) and the NRMSE were calculated using Equations 2 and 3 (Liu et al., 2012; Willmott, 1982).

$$RE = \frac{\overline{S} - \overline{O}}{\overline{O}} \quad (2)$$

$$NRMSE = RMSE/\overline{O} \times 100 = \sqrt{\frac{\sum_{i=1}^{n}(S_i - O_i)^2}{n}}\Big/\overline{O} \times 100 \quad (3)$$

where S_i, $\overline{S}$, O_i, $\overline{O}$, and n are the ith simulated values, the average of the simulated values, the ith observed values, the average of the observed values, and the number of observed values, respectively. The other calibration strategies (APP2, APP3, and APP4) employed the same objective function in the calibration and evaluation criteria as those of the APP1 case.

2.3. Scenario analysis

2.3.1. Streamflow

The water availability and irrigation application scenarios were developed based on the streamflow observations at the watershed outlet. Streamflow from the Courjolle River was monitored from August 2018 to March 2019. A water level sensor was installed along with a level staff close to the outlet on August 22, 2018 to record the water level every minute. The cross-section of the monitoring point and flow velocity were, on average, measured once a week. Based on the measurements, a rating curve was developed for the Courjolle River and then used to convert the recorded water levels to daily average discharge.

The baseflow separation was implemented to estimate the contribution of baseflow and direct runoff to the streamflow over time (Wittenberg, 1999). The recursive filter technique adopted in Baseflow Filter Program (or BFlow, https://swat.tamu.edu/media/70817/baseflow2006 -06.zip) was used to separate baseflow from total runoff (Arnold and Allen, 1999). The baseflow index (BFI), which represents the ratio of baseflow to the total runoff, was calculated to quantify the contribution of baseflow to the water resources. The Richards-Baker (R-B) flashiness index of the streamflow was calculated to understand the temporal dynamics of the river flow and the promptness of surface water responses to rainfall events in the watershed (Baker et al., 2004). Undeveloped (or natural) watersheds tend to have smaller R-B index values than developed (or urbanized) ones. Baker et al. (2004) reported that an index of 0.25 for a stream with a watershed area less than 77.7 km^2 would be classified in the stable groundwater-based streams, while the same R-B index (0.25) for a greater watershed (7770 km^2) would be considered as a flashy stream. They also found that a negative correlation could exist between the R-B Index with the baseflow and watershed area. During the hydrological monitoring, streamflow data contained missing values due to sensor malfunction, sedimentation at the station, and the limited capacity of a data logger

used. The missing streamflow level data were filled by the linear interpolation of available data.

2.3.2. Irrigation water availability

The daily discharge data obtained from the streamflow monitoring were converted into the daily volume to quantify the water availability for the downstream agricultural system as follows:

$$WA = SD * 60 * 60 * 24 * \mathcal{E}$$

where WA is the amount of water available for irrigation (m^3 day^{-1}), SD is the observed streamflow discharge (m^3 s^{-1}), $\mathcal{E}$ is the irrigation efficiency, and 60 and 24 are used as conversion factors from m^3 s^{-1} to m^3 day^{-1}. There are two types of the canal in this region, concrete (or lined) and earthen canals. The lined canal delivers water from the watershed outlet (or the dam) to each of the irrigation blocks that contain multiple dry bean fields. Then, water delivered to the entrance of each irrigation block is distributed to the individual fields through the earthen canal networks. In this study, an irrigation efficiency of 50 % was assumed based on the literature and knowledge of the local conditions (Brouwer et al., 1989). A local dry bean researcher (Raphael Colbert, personal communication) suggested that typically a fixed amount of irrigation water was applied every eight days. This estimated amount of water for irrigation was then used as an input for the dry bean model. The following equation was used to calculate the daily water availability in the unit of depth (mm) for the dry bean irrigation scenario:

$$WA_D = \frac{WA}{Area_{Irrigation} \times 10}$$

where WA_D is daily irrigation water available in mm and $Area_{Irrigation}$ is the size of the area that is being irrigated in ha (1800 ha in this study) (MARNDR, 2012), and 10 is a conversion factor from m^3 day^{-1} to mm day^{-1}. We then calculated the sum of the daily available water (WA_D) for the entire dry bean growing season, which lasts two and a half months.

2.3.3. Planting dates

The planting date for dry bean was determined based on the knowledge of management practices implemented in the study areas. The local farmers grow dry bean from December to March, which is called "*Campagne de haricot d'hiver*" (winter bean growing season). The farmers do not sow all seed at the same time due to the limited availability of seeds and the lack of sufficient labor. The data obtained from the Ministry of Agriculture of Haiti for the winter bean growing seasons in 2015 – 2016 and 2016 – 2017 showed that the sowing dates ranged from December 10 to January 15, but most of the planting dates were close to December 15. Since the yield responses to irrigation water deficits were the focus of this study, we assumed that fertilizer was not limiting and that pests, diseases, and weeds were properly controlled.

2.3.4. Scenario Development

Fifteen water availability and irrigation scenarios were developed from the combinations of planting dates and irrigation management practices. Five dates were selected for the planting season scenarios (i.e., October 15, November 15, December 15, January 15, and February 15). Three irrigation application scenarios were prepared: well-irrigated (Unlimited), irrigated under the currently available irrigation water (Limited)), and no irrigation water applied (Rainfed). In the scenario analysis, the water availability for irrigation under the current (limited irrigation water) condition was estimated from streamflow monitoring, as previously mentioned. The average length of a dry bean growing season is two and a half months (or 75 days). Thus, the amount of available water for irrigation during the growing season was calculated by summing the daily flow discharge as depth (mm) for the 75-day period. In the scenarios, dry bean fields were assumed to be irrigated once every eight days, which is the current water management practice implemented in the study area.

For the limited irrigation water condition, irrigation water measured for the 2018 – 2019 growing season was used as a reference to estimate the amount of water available from rainfall for the other thirty-five years from 1983 to 2018. The long-term irrigation water availability could be estimated from a calibrated hydrological model, which would provide the estimates of streamflow availability from the upstream watershed considering the watershed dynamics. However, there is no long-term station-based weather observation (only remotely-sensed rainfall and temperature estimates are available, such as NASA POWER rainfall) that can help to provide reliable hydrological modeling and streamflow prediction in this study. Thus, we decided to use a simple method to estimate the amount of water available for irrigation from the remotely-sensed rainfall estimates so as to avoid the introduction of unnecessary complexity and associated uncertainty into analysis results. In the simple method, the streamflow measured for the 2018–2019 growing season was used as a reference runoff and compared with the rainfall data for the same period of measurements to calculate monthly runoff-rainfall ratios or runoff coefficients (Acınan, 2008; Kadioglu and Şen, 2001; Karamage et al., 2018; Şen and Altunkaynak, 2006). Then, the ratios were applied to the rainfall data to estimate the corresponding amount of runoff considered as monthly water availability for the other thirty-five years to run the long-term simulations.

For the scenario analysis, the December 15 planting season was selected for the baseline scenario because it represents the current farming practice in the study areas (Table 3). The planting dates were then shifted to one or two months earlier (October and November) to include scenarios that can secure more irrigation water (wet period). The planting dates were also moved later to January 15 and February 15 to have scenarios with greater solar radiation and higher

Table 3
Planting and irrigation management scenarios.

Scenario Number	Scenario Name		
1	October Unlimited	October	Unlimited irrigation water (U)
2	October Limited	October	Limited irrigation water (L)
3	October Rainfed	October	Rainfed (R)
4	November Unlimited	November	Unlimited irrigation water (U)
5	November Limited	November	Limited irrigation water (L)
6	November Rainfed	November	Rainfed (R)
7	December Unlimited	December	Unlimited irrigation water (U)
8 (Baseline)	December Limited	December	Limited irrigation water (L)
9	December Rainfed	December	Rainfed (R)
10	January Unlimited	January	Unlimited irrigation water (U)
11	January Limited	January	Limited irrigation water (L)
12	January Rainfed	January	Rainfed (R)
13	February Unlimited	February	Unlimited irrigation water (U)
14	February Limited	February	Limited irrigation water (L)
15	February Rainfed	February	Rainfed (R)

Table 4
Summary of dry bean management practices represented in the CSM-CROPGRO-Dry bean model for the scenario analysis.

Components defined	Description
Planting date	October 15, November 15, December 15, January 15, and February 15
Field design	(1) Plant population at sowing date (plants/m^2): 16.67 (2) Plant population at emergence date (plants/m^2): 16.67 (3) Row spacing (cm): 60 (4) Planting depth (cm): 4
Fertilization	No fertilization
Initial soil conditions	(1) Previous crop: dry bean (2) Initial residue root weight (kg/ha): 1 (3) Initial nodule weight (kg/ha): 0 (4) Initial residue nitrogen (%): 0.5 (5) Initial residue phosphorus (%): 0.5 (6) Initial available soil water (%): 50 (7) Initial soil nitrogen (kg/ha): 25

temperature for dry bean growth. In the irrigation scenario analysis, the amount of water available was assumed to be evenly applied to all dry bean fields. For the long-term dry bean growth simulation, the information of dry bean management practices was compiled from local growers and researchers (Table 4).

In the case of the unlimited irrigation water scenarios, the amount of water supplied for irrigation was determined based on soil moisture simulated using the calibrated CSM- CROPGRO-Dry bean model. The soil profile was set to be fully refilled to its water-holding (or field) capacity within the depth of 30 cm (root zone) whenever the soil water content became equal to or less than 80 % of the capacity regardless of the water availability (Lopez et al., 2017). The rainfed scenarios assumed that no irrigation water was available or applied. Two such extreme scenarios, unlimited irrigation water (U) and rainfed (R), were introduced to demonstrate the yield response to irrigation in the study areas.

3. Results and discussion

3.1. Crop model calibration and evaluation

The performance of the calibrated CSM-CROPGRO Dry-bean model in predicting anthesis, maturity, and yield for dry bean was evaluated in terms of accuracy statistics, including RMSE, NRMSE, and RE (Table 5). The values for the cultivar coefficients for the variety X-RAV-40 estimated based on five calibration approaches are compared in Table 6. In the case of APP1 (COMB1 and COMB2), the calibrated model predicted anthesis and maturity on average within a 1-day error for both model calibration and evaluation. The simulated average flowering time was 38 days after sowing, which was the same as the observed value (38 days) and similar to the value (37 days) reported by the National Seed Service of the Ministry of Agriculture of Haiti (Beaver et al., 2014). The simulated number of days (68 days) from sowing to maturity was also similar to those (67 and 68 days) reported by the Ministry of Agriculture in 2017. The evaluation showed that the CSM-CROPGRO-Dry bean model could mathematically represent the physiological processes of dry bean for the study area in Haiti.

For the APP2 calibration approach, the dry bean phenology was simulated by the model with errors that were less than 2 days for both

Table 6
Genetic coefficients for the cultivar X-RAV-40 estimated using four calibration approaches.

Parameters	Range[10]	APP1-COMB1[11]	APP1-COMB2[12]	APP2	APP3	APP4
EM-FL[1]	20–35	31.4	32.1	30.9	33.2	30.8
FL-SD[2]	6–13	12.3	10.4	12.5	10.4	7.3
SD-PM[3]	14–29	14.9	16.0	14.5	15.1	17.8
SLAVR[4]	250–350	255	302	280	256	304
SIZLF[5]	133–180	140	135	139	141	138
WTPSD[6]	0.22–0.66	0.36	0.24	0.54	0.31	0.24
SFDUR[7]	11–22	21.9	21.2	21.4	20.8	11.9
SDPDV[8]	2–5	4.77	3.80	3.78	3.27	3.33
PODUR[9]	4–16	15.4	15.6	15.9	15.8	4.37

[1]Time between plant emergence and first flower (R1) (photothermal days); [2] Time between first flower and first seed (R5) (photothermal days); [3] Time between first seed (R5) and physiological maturity (R7) (photothermal days); [4] Specific leaf area under standard growth conditions (cm^2/g); [5] Maximum size of full leaf (three leaflets) (cm^2); [6] Maximum weight per seed (g); [7] Seed filling duration for pod cohort at standard growth conditions (photothermal days); [8] Average seed per pod under standard growing conditions (#/pod); [9] Time required for a cultivar to reach final pod load under optimal conditions (photothermal days); [10] The range for the genetic coefficients for the dry bean cultivar are adopted from the DSSAT Version 4.7.5 - (Hoogenboom et al., 2019a). [10] the first calibration approach with data combination 1; [11] the first calibration approach with data combination 2.

Table 5
Evaluation of the CSM-CROPGRO-Dry bean model for anthesis, maturity, and yield for the study area (Arcahaie, Haiti).

Variables	Calibration Approach	Calibration					Evaluation				
		Obs.[1]	Sim.[2]	RMSE[3]	NRMSE[4] (%)	RE[5] (%)	Obs.	Sim.	RMSE	NRMSE (%)	RE (%)
Anthesis (day)[6]	APP1-COMB1[9]	38	38	3.0	8.0	0.0	39	38	2.7	7.0	3.0
	APP1-COMB2[10]	39	39	2.7	6.9	0.0	38	39	3.2	8.3	3.0
	APP2	40	40	0.0	0.0	0.0	38	40	2.0	5.3	5.3
	APP3	38	38	0.0	0.0	0.0	43	41	2.0	4.7	3.0
	APP4	37	37	0.0	0.0	0.0	42	38	4.0	9.5	9.5
Maturity (day)[7]	APP1-COMB1	67	68	2.0	3.0	1.0	68	68	1.9	2.8	0.0
	APP1-COMB2	68	68	1.9	2.8	0.0	67	68	2.0	3.0	1.0
	APP2	66	67	2.0	3.0	1.5	68	68	0.0	0.0	0.0
	APP3	66	66	0.7	1.1	0.0	70	68	2.0	2.9	1.0
	APP4	63	63	0.0	0.0	0.0	70	65	5.0	7.1	7.1
Yield (kg/ha)[8]	APP1-COMB1	1,412	1,485	255	18.1	5.0	1,426	1,515	304	21.3	6.0
	APP1-COMB2	1,426	1,648	379	26.6	16.0	1,412	1,628	333	23.6	15.0
	APP2	932	1,465	533	57.2	57.2	1,329	1,599	270	20.3	20.3
	APP3	1,040	1,214	174	16.7	16.7	1,114	1,410	296	26.6	26.6
	APP4	950	1,601	651	68.5	68.5	1,655	1,484	171	10.3	10.3

[1] the mean values of the observed; [2] the mean values of the simulated; [3] root mean squared errors (RMSEs) of the simulated; [4] normalized RMSEs of the simulated; [5] relative errors of the simulated; [6] time to flowering; [7] time to physiological maturity; [8] dry bean yield at maturity; [9] the first calibration approach with data combination 1; [10] the first calibration approach with data combination 2.

calibration and evaluation. There was only one day of difference between the simulated and observed physiological maturity date (Table 5). For final the yield the simulations were not as accurate; the NRMSE for dry bean yield ranged from 20.3 % to 57.2 % for the calibration and the evaluation, which was considered as a poor performance (Jamieson et al., 1991; Rinaldi et al., 2003). The APP3 calibration approach provided a difference of 0 to 2 days in predicting the time to flowering (Table 5), while the NRMSE for yield prediction had a fair accuracy (16.7 % to 26.6 %). Thus, the genetic coefficients estimated based on the APP3 approach are the best candidates for application of the model and scenario analysis. In the case of APP4, the prediction errors for the time to flowering and physiological maturity ranged from 0 to 5 days for both calibration and evaluation (Table 5). The predicted yield ranged from 1,601 kg ha^{-1} and 1,484 kg ha^{-1}, which were 10.3 % to 68.5 % greater than the observed yield (950 kg ha^{-1} and 1,655 kg ha^{-1}).

For the APP2, APP3, and APP4 calibration approaches, the difference between the simulated and observed anthesis and maturity ranged from 2 to 5 days, which was worse compared to the accuracy provided by the APP1 calibration approach (Table 5). The largest differences in the anthesis (4 days) and maturity (5 days) were observed for the APP4 calibration approach. The observed time to flowering and physiological maturity was 42 and 70 days, respectively for the 2017 experiment. The APP4 calibration approach substantially underestimated both anthesis and physiological maturity with 37 days to anthesis for both 2016 and 2018 and 63 and 67 days to physiological maturity for the 2016 and the 2018 experiments.

In the case of the first calibration approach (APP1), the NRMSE of dry bean yield simulated from the first data combination (APP1-COMB1) and the second data combination (APP1-COMB2) ranged from 18 % to 27 % for model calibration and evaluation. These error statistics indicate that the CSM-CROPGRO-Drybean model provided a 'fair' performance when simulating the dry bean yield using the calibrated cultivar coefficients (Jamieson et al., 1991; Rinaldi et al., 2003). The predicted yield, i.e., 1515 kg ha^{-1} for APP1-COMB1 and 1628 kg ha^{-1} for APP1-COMB2, was greater than the observed yield, i.e., 1426 kg ha^{-1} for APP1–COMB1and 1,412 ha^{-1} for APP1-COMB2, and the differences (6 % and 15 %) were regarded as acceptable since the NRMSE was less than 30 %. The set of genetic coefficient values identified from the APP1-COMB1 was selected for the scenario analysis since the APP1-–COMB1 provided the best agreement with the observed values among the different calibration approaches (Tables 5 and 6).

The error in yield prediction increased from 5.0 % to 68.5 %, and from 6.0 % to 26.6 % during the calibration and the evaluation, respectively (Table 5). This can be explained by the variability in crop management practices and weather conditions that were not effectively captured by the weather data that were used for modeling as well as uncertainty in the observed yield data. In addition, the field experiments implemented in the study areas showed that variation in yield of different dry bean cultivars was larger than the variation in anthesis and physiological maturity (unpublished data, Raphael Colbert). For the three years of dry bean experiments there was only a one to three day of variation in anthesis, while observed yield fluctuated much more during the same period.

3.2. Temporal variation in the availability of irrigation water

The runoff hydrograph observed at the watershed outlet showed fluctuations in the flow rate from August to October with the average flowrate of 3.26 m^3 s^{-1} and peak discharges of 8.02 m^3 s^{-1} (on October 16) (Fig. 4). Baseflow started comprising a relatively large contribution to the streamflow in November although the baseflow started to decrease in October. The BFI was estimated to be 0.70, which indicates the significance of the baseflow as the source of water in the study areas. The R-B flashiness index for the monitoring period, including the wet and dry seasons, was 0.14, and was 0.21 when only the wet period was considered (August to October). Based on a total watershed area of 80 km^2, an R-B index of 0.14 indicates that the Courjolle River is a stable groundwater-based stream that has relatively significant and constant groundwater contribution to the streamflow (Baker et al., 2004). The baseflow separation and flashiness analysis showed that baseflow is the major source of agricultural water in the watershed.

Fig. 4. Streamflow hydrographs measured at the outlet of the watershed system (or the Courjolle river) from August 2018 to March 2019. The baseflow was separated from the total runoff using the BFlow method, and precipitation was recorded at a local weather station close to the study area.

The hydrograph analysis showed that streamflow could provide more water than required for dry bean irrigation for a portion of the rainy season (October and November) (Fig. 4 and Table 7). The amount of water available could be greater than that of rainfall in the two months due to the delayed contribution of baseflow to the total streamflow. In the limited irrigation water scenarios for the October planting dates (October Limited), therefore, irrigation water was not limited, which made the average amount of irrigation water applied for the simulation period of 35 years similar to each other in the unlimited and limited irrigation scenarios (October Unlimited vs. October Limited).

The CSM-CROPGRO-Dry bean model predicted that the irrigation requirement would increase by 37 % when changing the planting date from October to February under the unlimited irrigation scenarios (October Unlimited vs. February Unlimited) (Table 7). Such an increase can be explained by a decrease in rainfall and an increase in evapotranspiration (ET) from dry bean due to an increase in temperature and solar radiation (Tables 7 and 8). Thus, the amount of water available from the upstream watershed for dry bean irrigation became more critical when delaying the planting date.

3.3. Responses of evapotranspiration to water availability

The ET rates were sensitive to the irrigation management scenarios (Table 8). Crop water demand or crop evapotranspiration (ET) increased from the October planting scenario (dry bean started growing from October for two and a half months; Table 3) to the February (dry bean started growing from February for two and a half months; Table 3) constantly (Table 8). In this study, the potential (PET) was estimated based on the Priestley-Taylor equation, which expresses daily PET rates as a nonlinear function of daily solar radiation, air temperature, and relative humidity (Priestley and Taylor, 1972; Allen et al., 1998; Jones et al., 2003; Hoogenboom et al. 2019a, 2019b). The Priestley-Taylor expression can explain the ET increases from the October Unlimited to the February Unlimited scenarios. When water is fully available through irrigation and rainfall (the Unlimited scenarios), for instance, the crop water demand is essentially dependent on the weather conditions such as solar radiation and temperature.

The seasonal variation patterns of ET changed for the Limited water and Rainfed conditions. For the Rainfed situation, the water demand decreased from the October planting scenario (October Rainfed) to the December planting scenario (December Rainfed) and then increased from the December Rainfed to the February Rainfed scenarios (Table 8). Given that the only source of water was rainfall, dry bean ET followed the same pattern as that of the total rainfall amounts (Table 7 and Table 8). For the Rainfed scenarios, the actual crop ET was limited by a small amount of soil water in the dry season, which created drought stress affecting the leaf and canopy growth and dry matter production (Table 8; Boote et al., 2008; Dhakar et al., 2018; Jamieson et al., 1995; Saseendran et al., 2008).

In the case of the Limited condition, ET increased slightly from the October planting scenario (October Limited) to the November Limited (246 mm) and then decreased from the December Limited (219 mm) to the January Limited (149 mm) and then increased again for the February planting scenario (February Limited) (168 mm). This specific

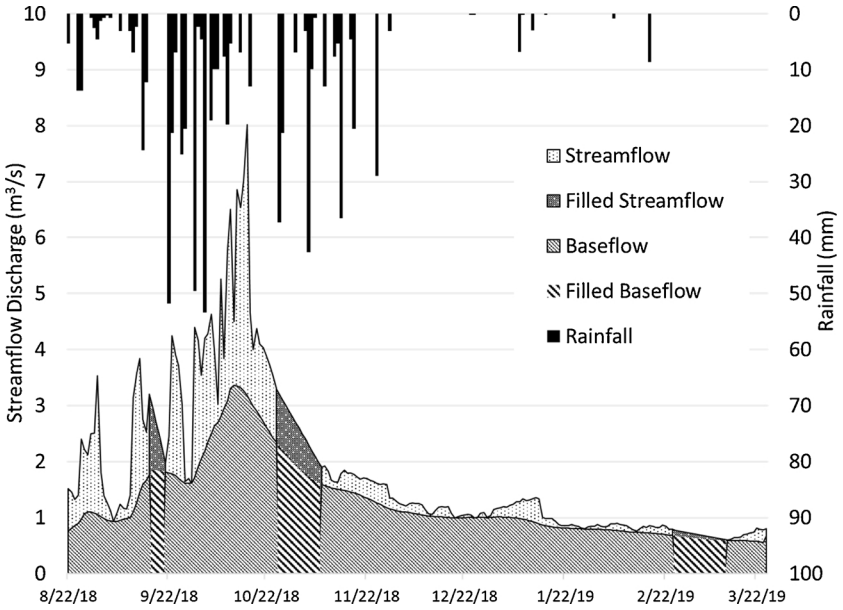

Fig. 4. Streamflow hydrographs measured at the outlet of the watershed system (or the Courjolle river) from August 2018 to March 2019. The baseflow was separated from the total runoff using the BFlow method, and precipitation was recorded at a local weather station close to the study areas.

Table 7
The amount of irrigation supplied to the dry bean fields, and the ranges of rainfall available for each scenario based on the NASA POWER rainfall data.

Scenario Number	Scenario Code	Mean and Range forf Irrigation (mm)	Rainfall range (mm)
1	October Unlimited	89–268 (185)	11–277
2	October Limited	89–268 (184)	
3	October Rainfed	0	
4	November Unlimited	114–271 (217)	10–254
5	November Limited	75–252 (191)	
6	November Rainfed	0	
7	December Unlimited	183–283 (242)	10–116
8 (Baseline)	December Limited	45–241 (161)	
9	December Rainfed	0	
10	January Unlimited	180–296 (253)	10–147
11	January Limited	12–178 (61)	
12	January Rainfed	0	
13	February Unlimited	175–306 (254)	11–203
14	February Limited	11–205 (73)	
15	February Rainfed	0	

Table 8
Summary of the median and coefficient of variation for simulated yield, daily average total solar radiation, maximum and minimum temperature, and evapotranspiration for each scenario using the NASAPOWER rainfall data.

Scenarios	Median Yield (kg/ha)	CV Yield (%)	SRAD (MJ/m^2)	Tmax (^{o}C)	Tmin (^{o}C)	ET (mm)
October Unlimited	1,246	13.1	16.2	30.4	21.9	250
October Limited	1,246	13.2				244
October Rainfed	49	146.1				132
November Unlimited	1,353	9.9	16.3	30.1	20.6	253
November Limited	1,303	38.1				246
November Rainfed	39	176.4				100
December Unlimited	1,447	9.2	17.4	30.3	20.1	268
December Limited	676	78.1				219
December Rainfed	33	41.4				87
January Unlimited	1,535	11.7	19.1	30.8	20.4	289
January Limited	55	184.7				149
January Rainfed	30	101.0				93
February Unlimited	1,538	11.7	20.6	31.5	21.3	304
February Limited	68	169.4				168
February Rainfed	36	101.0				106

CV: Coefficient of variation, SRAD: solar radiation, Tmax: maximum temperature, Tmin: minimum temperature, ET: evapotranspiration.

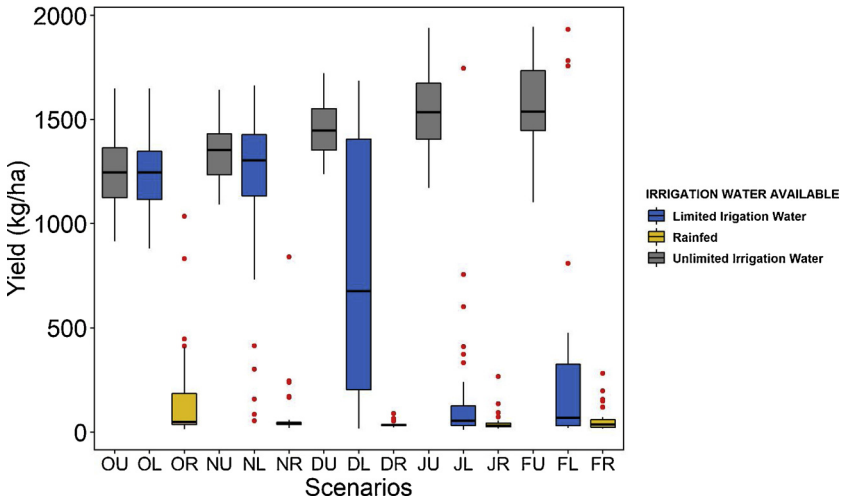

Fig. 5. Variability in simulated dry bean yield for the planting date and irrigation scenarios.

pattern for ET was because sufficient water based on a combination of irrigation and rainfall was available for the October Limited and November Limited scenarios. Then, ET followed the trend of seasonal solar radiation and air temperature from the October Limited to the November Limited scenarios, as found in the Unlimited condition (Table 8). For the dry season, solar radiation and temperature continued to increase while the available water for dry bean decreased during the dry season from December Limited to the February Limited scenarios, which affected ET, growth, and final yield (Tables 7 and 8).

3.4. Responses of dry bean yield to water availability

The long-term dry bean simulations showed that the rainfed scenarios (October Rainfed, November Rainfed, December Rainfed, January Rainfed, and February Rainfed) resulted in the lowest yield with the median ranging from 30 kg ha^{-1} (January Rainfed) to 49 kg ha^{-1} (October Rainfed) (Table 8 and Fig. 5). These findings highlight the importance of irrigation for dry bean production in the study area. Under rainfed conditions, the December Rainfed scenario resulted in the second-lowest median yield of 33 kg ha^{-1}, 8 % to 32 % less compared to those of the other scenarios. This was due to the smallest amount of rainfall received during the growing period of December Rainfed, December to March (47 mm) compared to October Rainfed (97 mm), November Rainfed (62 mm), January Rainfed (52 mm) and February Rainfed (74 mm) (Figs. 2,4, and 5).

Fig. 5. Variability in simulated dry bean yield for the planting date and irrigation scenarios

For the unlimited irrigated conditions, dry bean yield increased consistently from the October to the February planting scenario, which is not surprising since solar radiation and temperature increased during this period as well (Fig. 2 and Table 8). For instance, the yield for the February planting date (February Unlimited) was 23 % higher than that for the October planting date (October Unlimited). These findings indicate that solar radiation and temperature becomes a limiting factor for dry bean growth when irrigation water is not limited.

The simulated dry bean yield under the limited irrigation water scenarios (October Limited, November Limited, December Limited, January Limited, and February Limited) decreased consistently from the November (November Limited) to the February (February Limited) planting scenario (Fig. 5). This can be explained by the fact that the amount of irrigation water supplied by the river as well as rainfall significantly decreased from November to February (Figs. 2,4,5, and Table 7). For instance, if dry bean is planted in January and February (January Limited and February Limited), the model predicted that the yield would decrease by 92 % and 90 %, respectively, compared to that of December Limited. On the other hand, yield was predicted to increase by 84 % and 93 %, respectively, for the October Limited and November Limited scenarios, compared to that of the December Limited scenario. These simulation results demonstrate that the productivity of the agricultural area is significantly limited by both the amount and the temporal variability of the water that is provided by the upstream watershed. In addition, these findings imply that the availability of irrigation is more critical to dry bean production than the effect of solar radiation and temperature in the study area. The scenario analysis results suggest that local farmers can plant dry bean earlier than December to improve their yield if they are able to secure more water from the river for supplemental irrigation.

3.5. Implications and limitations

This study demonstrated that the productivity of a downstream irrigation district relies on the upstream hydrological processes and the seasonal variability of these hydrological processes. The baseflow separation analysis showed that streamflow of the study watershed mainly consisted of baseflow, e.g., BFI of 0.70 and the R-B flashiness index of 0.14, especially during the dry months, which indicates that the watershed is a groundwater-based system (Baker et al., 2004). These hydrologic features are favored for the purpose of irrigation as groundwater discharge or baseflow is more consistent compared to direct runoff, providing a more stable water supply for irrigation. The water availability and irrigation scenario analyses suggest that the agricultural productivity can be improved by securing baseflow from the watershed, which can be accomplished by the reforestation of the savannah regions in the upstream drainage areas and watershed of the irrigation district (Filoso et al., 2017; Ilstedt et al., 2016).

Dry bean yield can also be improved by reducing water loss during conveyance from the river to the field, while proper maintenance of the irrigation water delivery system can help increase the amount of water available for irrigation. The use of advanced irrigation scheduling methods, such as determining the amount and timing of water application based on the information of soil water conditions and growing stages, can help local farmers save water resources under the current limited water availability condition without a large investment in the existing irrigation system (Liang et al., 2016; Lopez et al., 2017). An optimum water application schedule also can be identified from both experimental and simulation studies such as modeling analysis of this study, which could be an interesting subject for future research.

One of the greatest challenges of this study was the limited quantity and quality of experimental data that were available for crop modeling and scenario analysis. Crop modeling requires at least local rainfall

data, especially for tropical environments (Hoogenboom, 2000a). However, the local weather data had many missing days, and there was no local weather record that could help to analyze the long-term weather and hydrologic variability. Thus, the weather input data for the crop modeling had to be complemented with the remotely sensed rainfall estimates that are known to have much uncertainty, which in turn could affect the irrigation water availability estimates (Awange et al., 2016; McMillan et al., 2018). In addition, the crop model was calibrated to measurements that are potentially biased (towards a relatively low yield). The crop growth and yield observations were obtained from field experiments that imposed nutrient stresses on crops, which were only measurements that could show the physiological characteristics of dry bean in the study area. The streamflow had been monitored for only nine months due to the limited accessibility to the area. Although the monitoring period includes the growing seasons of dry bean, the streamflow data had to be extrapolated to estimate irrigation availability from the relationship between runoff discharges and rainfall depths observed during the monitoring period. The imperfect measurements and the subsequent uncertainty introduced during the hydrologic analysis and crop model calibration should affect outputs of the scenario analysis (Harmel et al., 2006; Hoogenboom, 2000). However, this study emphasized the relative comparison between the efficiency of irrigation and dry bean management practices, while uncertainty will be considered in a future study.

3.6. Conclusion

The crop modeling experiment demonstrated that dry bean production with the traditional mid-December planting date was substantially reduced by a limited availability of irrigation. In addition, streamflow monitoring indicated that irrigation water availability would decrease as dry bean planting was delayed. These findings suggest that local farmers should plant dry bean earlier to be able to procure more irrigation water that could results in an increase in yield. It also implies that securing more stable water resources such as baseflow other than direct runoff can help improve dry bean production. This study demonstrated that agricultural production could benefit from integrated knowledge of the relationship between physically separated but hydrologically connected areas, the upstream watershed and downstream irrigation district. Such knowledge highlights the need for a science-based and coordinated approach to natural resources management in improving agricultural productivity and sustainability.

Declaration of Competing Interest

The authors declare that they have no known competing financial interests or personal relationships that could have appeared to influence the work reported in this paper.

Acknowledgments

This study was financially supported by Feed the Future USAID-Haiti, and the award number is AID-OAA-A-15-00039. The authors acknowledge (1) Agr. Gasner Démosthène and Jasson Innovil from the Ministry of Agriculture of Haiti for sharing the dry bean data sets and (2) Agr. Banel Sydne and Agr. Abdias S.V. Pierre for sharing the historical flow monitoring data. Long-term daily weather data were obtained from the NASA Langley Research Center (LaRC) POWER Project funded through the NASA Earth Science/Applied Science Program.

References

Acınan, S., 2008. Determination of Runoff Coefficient of Basins by Using Geographic Information Systems. Middle East Technical University, Ankara, Turkey.

Allen, R.G., Pereira, L.S., Raes, D., Smith, M., 1998. Crop evapotranspiration: Guidelines for Computing Crop Water Requirements. Irrigation and Drainage Paper No. 56. FAO, Rome Available at:Accessed 03 July 2020. http://www.fao.org/3/x0490e/x0490e0e.htm.

Alvarez, J., Nuthall, P., 2006. Adoption of computer based information systems: The case of dairy farmers in Canterbury, NZ, and Florida, Uruguay. Comput. Electron. Agric. 50, 48–60. https://doi.org/10.1016/j.compag.2005.08.013.

Anar, M.J., Lin, Z., Hoogenboom, G., Shelia, V., Batchelor, W.D., Teboh, J.M., Ostlie, M., Schatz, B.G., Khan, M., 2019. Modeling growth, development and yield of Sugarbeet using DSSAT. Agric. Sys. 169, 58–70. https://doi.org/10.1016/j.agsy.2018.11.010.

Arnold, J.G., Allen, P.M., 1999. Automated methods for estimating baseflow and ground water recharge from streamflow records. J. Am. Water. Resour. Assoc. 35, 411–424. https://doi.org/10.1111/j.1752-1688.1999.tb03599.x.

Awange, J.L., Ferreira, V.G., Forootan, E., Khandu, Andam-Akorful, S.A., Agutu, N.O., He, X.F., 2016. Uncertainties in remotely sensed precipitation data over Africa. Int. J. Climatol. 36, 303–323. https://doi.org/10.1002/joc.4346.

Baker, D.B., Richards, R.P., Loftus, T.T., Kramer, J.W., 2004. A new flashiness index: characteristics and applications to Midwestern rivers and streams. JAWRA. 40, 503–522. https://doi.org/10.1111/j.1752-1688.2004.tb01046.x.

Beaver, J., Prophete, E., Rosas, J., Godoy Lutz, G., Steadman, J., Porch, T., 2014. Release of "XRAV-40-4" Black bean (Phaseolus vulgaris L.) cultivar. J. Agri. Univ. Puerto Rico 98, 83–87. https://revistas.upr.edu/index.php/jaupr/article/view/224/222.

Belmar, O., Barquín, J., Álvarez-Martínez, J.M., Peñas, F.J., Del Jesus, M., 2016. The role of forest maturity on catchment hydrologic stability. Hydrol. Eart. Syst. Sci. Dis. 1–17. https://doi.org/10.5194/hess-2016-471.

Boote, K.J., Jones, J.W., Batchelor, W.D., Nafziger, E.D., Myers, O., 2003. Genetic coefficients in the CROPGRO-Soybean model: Links to field performance and genomics. Agron. J. 95, 32–51.

Boote, K.J., Sau, F., Hoogenboom, G., Jones, J.W., 2008. Experience with water balance, evapotranspiration, and predictions of water stress effects in the CROPGRO model. In: Ahuja, L.R., Reddy, V.R., Saseendran, S.A., Yu, Q. (Eds.), Response of Crops to Limited Water: Understanding and Modeling Water Stress Effect on Plant Growth Processes. Advances in Agricultural Systems Modeling Series 1, ASA, CSSA, SSSA, Madison, WI, pp. 59–103.

Brodt, S., Six, J., Feenstra, G., Ingels, C., Campbell, D., 2011. Sustainable agriculture. Nat. Edu. Knowledge 3 (10), 1.

Buddhaboon, C., Jintrawet, A., Hoogenboom, G., 2018. Methodology to estimate rice genetic coefficients for the CSM-CERES-Rice model using GENCALC and GLUE genetic coefficient estimators. J. Agri. Sci. 156, 482–492. https://doi.org/10.1017/S0021859618000527.

Dhakar, R., Sarath Chandran, M.A., Nagar, S., Visha Kumari, V., Subbarao, A.V.M., Bal, S.K., Vijaya Kumar, P., 2018. Field crop response to water deficit stress: assessment through crop models. In: Bal, S.K., Mukherjee, J., Choudhury, B.U., Dhawan, A.K. (Eds.), Advances in Crop Environment Interaction. Springer, Singapore, pp. 287–315. https://doi.org/10.1007/978-981-13-1861-0_11.

de Oliveira, E.C., Costa, J., José de, P.J., Ferreira, W., Justino, F., Neves, L., 2012d. The performance of the CROPGRO model for bean (Phaseolus vulgaris L.) yield simulation. Acta Scientiarum Agron. 34, 239–246. https://doi.org/10.4025/actasciagron.v34i3.13424.

Dieter, C.A., 2018. Water Availability and Use Science Program: Estimated Use of Water in the United States In 2015. Geol. Surv.

Dinku, T., Funk, C., Peterson, P., Maidment, R., Tadesse, T., Gadain, H., Ceccato, P., 2018. Validation of the CHIRPS satellite rainfall estimates over eastern Africa. Q. J. R. Meteorol. Soc. 144, 292–312. https://doi.org/10.1002/qj.3244.

Duan, K., Sun, G., Caldwell, P.V., McNulty, S.G., Zhang, Y., 2018. Implications of upstream flow availability for watershed surface water supply across the conterminous united states. J. Am. Water. Resour. Assoc. 54, 694–707. https://doi.org/10.1111/1752-1688.12644.

FAO, 2019. FAOSTAT - Crops [WWW Document]. Crops. URL. http://www.fao.org/faostat/en/#data/QC.

FAO, 2017. Water for Sustainable Food and Agriculture: A Report Produced for The G20 Presidency of Germany. FAO, Rome.

FAO, 2011. The State of the World's Land and Water Resources for Food and Agriculture. Rome, Italy. .

FAO-UNESCO, 2003. Digital Soil Map of the World and Derived Soil Properties [electronic resource] / FAO. UNESCO, Version 3. ed.. FAO, Rome.

FEWS, N.E.T., 2018. Haiti: Staple Food Market Fundamentals, March 2018. FEWS N.E.T.Haiti: Staple Food Market Fundamentals, March 2018. FEWS N.E.T.

Filoso, S., Bezerra, M.O., Weiss, K.C.B., Palmer, M.A., 2017. Impacts of forest restoration on water yield: A systematic review. PLoS One 12, e0183210. https://doi.org/10.1371/journal.pone.0183210.

Funk, C., Peterson, P., Landsfeld, M., Pedreros, D., Verdin, J., Shukla, S., Husak, G., Rowland, J., Harrison, L., Hoell, A., Michaelsen, J., 2015. The climate hazards infrared precipitation with stations—a new environmental record for monitoring extremes. Sci. Data 2, 150066. https://doi.org/10.1038/sdata.2015.66.

Gao, Y., Wallach, D., Liu, B., Dingkuhn, M., Boote, K.J., Singh, U., Asseng, S., Kahvech, T., He, J., Zhang, R., Confalonieri, R., Hoogenboom, G., 2020. Comparison of three calibration methods for modeling rice phenology. Agri. Forest Meteorol. 280 (2020), 107785. https://doi.org/10.1016/j.agrformet.2019.107785.

Gashaw, T., Tulu, T., Argaw, M., Worqlul, A., 2017. Evaluation and prediction of land use/land cover changes in the Andassa watershed, Blue Nile Basin, Ethiopia. Environ. Syst. Res. 6, 1–15. https://doi.org/10.1186/s40068-017-0094-5.

Gebremicael, T.G.G., Mohamed, Y.A.A., Van der Zaag, P., 2019. Attributing the hydrological impact of different land use types and their long-term dynamics through combining parsimonious hydrological modelling, alteration analysis and PLSR analysis. Sci. Total Environ. 660, 1155–1167. https://doi.org/10.1016/j.scitotenv.2019.01.085.

Gornall, J., Betts, R., Burke, E., Clark, R., Camp, J., Willett, K., Wiltshire, A., 2010.

Implications of climate change for agricultural productivity in the early twenty-first century. Philos. Trans. R. Soc. Lond. B Biol. Sci. 365, 2973–2989. https://doi.org/10.1098/rstb.2010.0158.
Guan, K., Sultan, B., Biasutti, M., Baron, C., Lobell, D.B., 2015. What aspects of future rainfall changes matter for crop yields in West Africa? Geophys. Res. Lett. 42, 8001–8010. https://doi.org/10.1002/2015GL063877.
Harmel, R.D., Cooper, R.J., Slade, R.M., Haney, R.L., Arnold, J.G., 2006. Cumulative uncertainty in measured streamflow and water quality data for small watersheds. Trans. ASABE 49, 689–701.
He, J., Dukes, M.D., Jones, W., Graham, W.D., Judge, J., 2009. Applying GLUE for Estimating CERES-Maize Genetic and Soil Parameters for Sweet Corn Production. Trans. ASABE 52, 1907–1921. https://doi.org/10.13031/2013.29218.
He, J., Jones, J.W., Graham, W.D., Dukes, M.D., 2010. Influence of likelihood function choice for estimating crop model parameters using the generalized likelihood uncertainty estimation method. Agri. Syst. 103, 256–264. https://doi.org/10.1016/j.agsy.2010.01.006.
Hoogenboom, G., 2000. Contribution of Agrometeorology to the Simulation of Crop Production and its Applications. 103. pp. 137–157 https://doi.org/DOI:10.1016/S0168-1923(00)00108-8.
Hoogenboom, G., Jones, J.W., Wilkens, P.W., Batchelor, W.D., Bowen, W.T., Hunt, L.A., Pickering, N.B., Singh, U., Godwin, D.C., Baer, B., Boote, K.J., Ritchie, J.T., White, J.W., 1994. Crop Models. In: Tsuji, G.Y., Uehara, G., Balas, S. (Eds.), DSSAT Version 3, Vol. 2. University of Hawaii, Honolulu, HI, pp. 95–244.
Hoogenboom, G., Porter, C.H., Shelia, V., Boote, K.J., Singh, U., White, J.W., Hunt, L.A., Ogoshi, R., Lizaso, J.I., Koo, J., Asseng, S., Singels, A., Moreno, L.P., Jones, J.W., 2019a. Decision Support System for Agrotechnology Transfer (DSSAT) Version 4.7.5 (https://DSSAT.net). DSSAT Foundation, Gainesville, Florida, USA.
Hoogenboom, G., Porter, C.H., Boote, K.J., Shelia, V., Wilkens, P.W., Singh, U., White, J.W., Asseng, S., Lizaso, J.I., Moreno, L.P., Pavan, W., Ogoshi, R., Hunt, L.A., Tsuji, G.Y., Jones, J.W., 2019b. The DSSAT crop modeling ecosystem. In: Boote, K.J. (Ed.), editor Advances in crop modeling for a sustainable agriculture. Burleigh Dodds Science Publishing, Cambridge, United Kingdom, pp. 173–216 (https://doi.org/10.19103/AS.2019.0061.10).
Hunt, L.A., White, J.W., Hoogenboom, G., 2001. Agronomic data: advances in documentation and protocols for exchange and use. Agri. Syst. 70, 477–492. https://doi.org/10.1016/S0308-521X(01)00056-7.
ICID, 2017. Irrigated Agriculture Development Under Drought and Water Scarcity. ICID, New Delhi, India.
Ilstedt, U., Bargués Tobella, A., Bazié, H.R., Bayala, J., Verbeeten, E., Nyberg, G., Sanou, J., Benegas, L., Murdiyarso, D., Laudon, H., Sheil, D., Malmer, A., 2016. Intermediate tree cover can maximize groundwater recharge in the seasonally dry tropics. Sci. Rep. 6, 21930. https://doi.org/10.1038/srep21930.
Inozile, J.W., 2016. Effet de la fertilisation et de l'inoculation sur le rendement et la nodulation de trois variétés de haricot à Cabaret. (Bachelor Thesis). Université Quisqueya.
Jamieson, P.D., Porter, J.R., Wilson, D.R., 1991. A test of the computer simulation model ARCWHEAT1 on wheat crops grown in New Zealand. Field Crop Res. 27, 337–350. https://doi.org/10.1016/0378-4290(91)90040-3.
Jeune, W., 2015. Solos e ambientes no Haiti ocidental: Gênese, classificação e mapeamento (PhD Thesis). Universidade Federal de Viçosa.
Jones, C.A., Kiniry, J.R., Dyke, P.T., 1986. CERES-Maize: A simulation model of maize growth and development, First edition. Texas A & M University Press, College Station.
Jones, J.W., He, J., Boote, K.J., Wilkens, P., Porter, C.H., Hu, Z., 2011. Estimating DSSAT cropping system cultivar-specific parameters using bayesian techniques. In: Ahuja, L.R., Ma, L. (Eds.), Methods of Introducing System Models into Agricultural Research (Advances in Agricultural Systems Modeling). American Society of Agronomy, Inc., United States of America, pp. 365–393.
Jones, J.W., Hoogenboom, G., Porter, C.H., Boote, K.J., Batchelor, W.D., Hunt, L.A., Wilkens, P.W., Singh, U., Gijsman, A.J., Ritchie, J.T., 2003. The DSSAT cropping system model. Eur. J. Agron. 18, 235–265. https://doi.org/10.1016/S1161-0301(02)00107-7.
Kadioglu, M., Şen, Z., 2001. Monthly precipitation-runoff polygons and mean runoff coefficients. Hydrolog. Sci. J. 46, 3–11. https://doi.org/10.1080/02626660109492796.
Karamage, F., Liu, Yuanbo, Fan, X., Francis Justine, M., Wu, G., Liu, Yongwei, Zhou, H., Wang, R., 2018. Spatial relationship between precipitation and runoff in africa. Hydrol. Earth Syst. Sc. Disc. 1–27. https://doi.org/10.5194/hess-2018-424.
Klemeš, V., 1986. Operational testing of hydrological simulation models. Hydrolog. Sci. J. 31, 13–24. https://doi.org/10.1080/02626668609491024.
Laraus, J., 2004. The problems of sustainable water use in the Mediterranean and research requirements for agriculture. Ann. Appl. Biol. 144, 259–272. https://doi.org/10.1111/j.1744-7348.2004.tb00342.x.
Liang, X., Liakos, V., Wendroth, O., Vellidis, G., 2016. Scheduling irrigation using an approach based on the van Genuchten model. Agric. Water Manag. 176, 170–179. https://doi.org/10.1016/j.agwat.2016.05.030.
Liu, H., Yang, Jing-yi, He, P., Bai, Y., Jin, J., Drury, C.F., Zhu, Y., Yang, X., Li, W., Xie, J., Yang, Jing-min, Hoogenboom, G., 2012. Optimizing parameters of CSM-CERES-Maize model to improve simulation performance of maize growth and nitrogen uptake in Northeast China. J. Integr. Agric. 11, 1898–1913. https://doi.org/10.1016/S2095-3119(12)60196-8.
Lopez, J.R., Winter, J.M., Elliott, J., Ruane, A.C., Porter, C., Hoogenboom, G., 2017. Integrating growth stage deficit irrigation into a process based crop model. Agric. For. Meteorol. 243, 84–92. https://doi.org/10.1016/j.agrformet.2017.05.001.
Maldonado, W., Valeriano, T.T.B., de Souza Rolim, G., 2019. EVAPO: A smartphone application to estimate potential evapotranspiration using cloud gridded meteorological data from NASA-POWER system. Comput. Electron. Agric. 156, 187–192. https://doi.org/10.1016/j.compag.2018.10.032.
MARNDR, 2012. Politique D'irrigation du MARNDR 2012-2016. Ministère de l'Agriculture des Ressources Naturelles et du Développement Rural. Port-au-Prince, Haiti.
McCown, R.L., 2002. Changing systems for supporting farmers' decisions: problems, paradigms, and prospects. Agric. Syst. 74, 179–220. https://doi.org/10.1016/S0308-521X(02)00026-4.
McMillan, H.K., Westerberg, I.K., Krueger, T., 2018. Hydrological data uncertainty and its implications. WIREs Water 5, e1319. https://doi.org/10.1002/wat2.1319.
McNider, R.T., Handyside, C., Doty, K., Ellenburg, W.L., Cruise, J.F., Christy, J.R., Moss, D., Sharda, V., Hoogenboom, G., Caldwell, P., 2015. An integrated crop and hydrologic modeling system to estimate hydrologic impacts of crop irrigation demands. Environ. Model. Softw. 72, 341–355. https://doi.org/10.1016/j.envsoft.2014.10.009.
Molnar, J.J., Kokoye, S., Jolly, C., Shannon, D.A., Huluka, G., 2015. Agricultural development in northern Haiti: Mechanisms and means for moving key crops forward in a changing climate. J. Agric. Environ. Sci. 4 (2), 17. https://doi.org/10.15640/jaes.v4n2a4.
Nepal, S., Flügel, W.-A., Shrestha, A., 2014. Upstream-downstream linkages of hydrological processes in the Himalayan region. Ecol. Processes 3, 1–16. https://doi.org/10.1186/s13717-014-0019-4.
OECD, 2017. Water Risk Hotspots for Agriculture (Text). OECD Studies on Water, Paris.
Olayide, O.E., Tetteh, I.K., Popoola, L., 2016. Differential impacts of rainfall and irrigation on agricultural production in Nigeria: Any lessons for climate-smart agriculture? Agric. Water Manag. 178, 30–36. https://doi.org/10.1016/j.agwat.2016.08.034.
Peel, M.C., Finlayson, B.L., McMahon, T.A., 2007. Updated world map of the Köppen-Geiger climate classification. Hydrol. Earth Syst. Sci. Disc. 4, 439–473. https://doi.org/10.5194/hessd-4-439-2007.
Priestley, C.H.B., Taylor, R.J., 1972. On the assessment of surface heat flux and evaporation using large-scale parameters. Month. Weather Rev. https://doi.org/10.1175/1520-0493(1972)100<0081:otaosh>2.3.co;2. 100:81-92.
Rinaldi, M., Losavio, N., Flagella, Z., 2003. Evaluation and application of the OILCROP–SUN model for sunflower in southern Italy. Agric. Syst. 78, 17–30. https://doi.org/10.1016/S0308-521X(03)00030-1.
Santos, M.G.D., Faria, R.T.D., Palaretti, L.F., Dantas, G.D.F., Dalri, A.B., Lopes, A.D.S., 2016. Calibration and testing of CS-CROPGRO model for common beans. Eng. Agric. 36, 1239–1249. https://doi.org/10.1590/1809-4430-eng.agric.v36n6p1239-1249/2016.
Saseendran, S.A., Ahuja, L.R., Ma, L., Timlin, D., Stöckle, C.O., Boote, K.J., Hoogenboom, G., 2008. Current water deficit stress simulations in selected agricultural system models. In: Ahuja, L.R., Reddy, V.R., Saseendran, S.A., Yu, Q. (Eds.), Response of Crops to Limited Water: Understanding and Modeling Water Stress Effect on Plant Growth Processes. Advances in Agricultural Systems Modeling Series 1, ASA, CSSA, SSSA, Madison, WI, pp. 1–38.
Sayer, J., Cassman, K.G., 2013. Agricultural innovation to protect the environment. Proc. Nat. Acad. Sci. 110, 8345–8348.
Şen, Z., Altunkaynak, A., 2006. A comparative fuzzy logic approach to runoff coefficient and runoff estimation. Hydrol. Proc. 20, 1993–2009. https://doi.org/10.1002/hyp.5992.
Shackelford, G.E., Kelsey, R., Sutherland, W.J., Kennedy, C.M., Wood, S.A., Gennet, S., Karp, D.S., Kremen, C., Seavy, N.E., Jedlicka, J.A., Gravuer, K., Kross, S.M., Bossio, D.A., Muñoz-Sáez, A., LaHue, D.G., Garbach, K., Ford, L.D., Felice, M., Reynolds, M.D., Rao, D.R., Boomer, K., LeBuhn, G., Dicks, L.V., 2019. Evidence synthesis as the basis for decision analysis: A method of selecting the best agricultural practices for multiple ecosystem services. Front. Sustain. Food Syst. 3. https://doi.org/10.3389/fsufs.2019.00083.
Stackhouse, P.W.J., Zhang, T., Westberg, D., Barnett, A.J., Bristow, T., Macpherson, B., Hoell, J.M., 2018. POWER Release 8.0.1 (with GIS Applications) Methodology (Data Parameters, Sources, & Validation).
Stubbs, M., 2016. Irrigation in U.S. Agriculture: On-Farm Technologies and Best Management Practices [October 17, 2016].
Sun, G., McNulty, S.G., Lu, J., Amatya, D.M., Liang, Y., Kolka, R.K., 2005. Regional annual water yield from forest lands and its response to potential deforestation across the southeastern United States. J. Hydrol. 308, 258–268. https://doi.org/10.1016/j.jhydrol.2004.11.021.
Thornton, P.K., Hoogenboom, G., 1994. A computer program to analyze single-season crop model outputs. Agron. J. 86, 860–868. https://doi.org/10.2134/agronj1994.00021962008600050020x.
USAI/MARNDR, 2016. Résultats des Enquêtes Nationales de la Production Agricole, Année 2016. Port-au-Prince, Haiti.
USGS, 2019. USGS EROS Archive - Digital Elevation - Shuttle Radar Topography Mission (SRTM) 1 Arc-Second Global.
Wallender, W., Grismer, M., 2002. Irrigation hydrology: Crossing scales. J. Irrig. Drain. Eng. 128, 203–211. https://doi.org/10.1061/(ASCE)0733-9437(2002)128:4(203).
Wang, G., Mang, S., Cai, H., Liu, S., Zhang, Z., Wang, L., Innes, J.L., 2016. Integrated watershed management: evolution, development and emerging trends. For. Res. 27, 967–994. https://doi.org/10.1007/s11676-016-0293-3.
White, J.W., Hoogenboom, G., Stackhouse, P.W., Hoell, J.M., 2008. Evaluation of NASA satellite- and assimilation model-derived long-term daily temperature data over the continental US. Agric. For. Meteorol. 148, 1574–1584. https://doi.org/10.1016/j.agrformet.2008.05.017.
Willmott, C.J., 1982. Some comments on the evaluation of model performance. Bull. Am. Meteorol. Soc. 63, 1309–1313 https://doi.org/SCOTEO&2.0.CO;2.
Winter, T.C., Harvey, J.W., Franke, O.L., Alley, W.M., 1998. Ground water and surface water; a single resource (USGS Numbered Series No. 1139), Circular. U.S. Geological Survey.

Wittenberg, H., 1999. Baseflow recession and recharge as nonlinear storage processes. Hydrol. Process. 13, 715–726. https://doi.org/10.1002/(SICI)1099-1085(19990415)13:5<715::AID-HYP775>3.0. CO;2-N.

Yang, H., Zehnder, A.J.B., 2002. Water scarcity and food import: A case study for southern mediterranean countries. World Dev. 30, 1413–1430. https://doi.org/10.1016/S0305-750X(02)00047-5.

Yoon, T., Rhodes, C., Shah, F.A., 2015. Upstream water resource management to address downstream pollution concerns: A policy framework with application to the Nakdong River basin in South Korea. Water Resour. Res. 51, 787–805. https://doi.org/10.1002/2013WR014201.